Elastomers and Composites
Vol. 58, No. 1 pp. 1~10 (March 2023)

Online ISSN 2288-7725
DOI: https://doi.org/10.7473/EC.2023.58.1.1

Vertical Alignment of Liquid Crystal on Film of Plant-based Polysaccharide Derivatives

Yeonsu Cho†, Jihyeon Moon†, DaEun Yang, and Hyo Kang†

Department of Chemical Engineering, Dong-A University, 37 Nakdong-Daero 550 Beon-Gil, Saha-Gu, Busan 49315, Republic of Korea

(Received December 7, 2022, Revised December 13, 2022, Accepted December 23, 2022)

Abstract: In this study, we investigate the liquid crystal (LC) alignment of LC cells created from plant-based polysaccharide derivatives, such as guar gum. Guar gum films exhibit satisfactorily high optical transparency in the visible light region (400-750 nm). For example, the transmittance of polyimide films, which are the most typically used LC alignment layers, is 87%, whereas that of guar gum films deposited onto a glass substrate at a wavelength of 550 nm is approximately 99%. The observed LC alignment depends on the rubbing depth. For example, an LC cell comprising a guar gum film fabricated via rubbing at rubbing depths of 0.1, 0.2, 0.3, and 0.4 mm exhibits a planar LC alignment, whereas it exhibits a vertical LC alignment at a rubbing depth of 0.5 mm. Additionally, the LC alignment is shown to be correlated with the total surface energy of the guar gum films. When the total surface energy of a rubbed guar gum film exceeds 58.10 mJ/m^2, an LC cell comprising the guar gum film exhibits a stable and vertical LC alignment. Therefore, guar gum can be used to realize the vertical alignment system of LC via a simple adjustment of the rubbing depth.

Keywords: liquid crystal, alignment, vertical, polysaccharide

Introduction

Liquid crystal (LC) molecules have been extensively investigated because they exhibit a unique property which is the existence of an intermediate phase between the solid and liquid phases. [1] LC molecules have been known to exhibit anisotropic physico-chemical characteristics such as optical anisotropy and dielectric anisotropy induced by external stimuli because of their unique chemical structures.[2] Owing to the discovery of LC molecules, remarkable progress has been achieved in diverse fields such as information technology,[3-5] nanotechnology,[6] biotechnology,[7] energy and environment technology[8,9] using interesting physico-chemical characteristics. Moreover, LC alignment technologies have been recognized as an interesting topic both academically and technologically for a long time. Techniques for aligning LCs in one direction are considerably important in LC applications.[10] For example, LC alignment technologies have been extensively used in the display industry in transmissive modes using nematic LCs and in reflective modes using cholesteric LCs.[10] Because LCs can change their optical characteristics in response to electrical signals to create text and images, they are an important component of displays.[11] Apart from display industry, more specifically, there are the various the application field of LC molecules, including electronics and photonics fields such as lenses,[12-15] energy fields such as secondary battery short circuit[16,17] and photovoltaics,[18-21] and biomedical fields such as drug delivery systems[22-26] and biochemical sensor.[27-30]

Mechanical rubbing of polymeric surfaces is the most widely used technique to achieve a uniform alignment of the LC molecules in the manufacture of liquid crystal displays (LCDs).[31-36] For the experiment, mechanical rubbing on polymeric substrates was achieved to fabricate a LCD panel. Microgrooves and/or scratches on polymeric surfaces were created by mechanical rubbing, which can align the LC molecules along the grooves and/or scratches to minimize the energy of elastic distortion.[37] Furthermore, it has been suggested that polymer chains are reoriented on the substrate, whereupon the LC molecules are aligned due to the intermolecular interactions between the polymer chains and LC molecules.[38] In particular, the mechanical rubbing method is strongly favored due to its advantages of mass productivity

†Corresponding author E-mail: hkang@dau.ac.kr
‡The authors contributed equally to this work.

and large area treatment of polymeric films.[39] Properties of LC alignment on polyimide surfaces have been reported previously.[40-46] Polyimide derivatives have been most generally used as LC alignment layers through mechanical rubbing, because they provide significantly stable LC alignments.[10,47-55] Polyimide derivatives exhibiting long alkyl or alkyloxy groups, such as semi-flexible copolyimides containing *n*-octadecyl side groups and polyimides containing (*n*-decyloxy)biphenyloxy side groups, exhibit vertical LC alignment behaviors.[56,57] Polystyrene (PS) derivatives exhibiting long alkyl chains can also produce vertical LC alignment layers. For example, LC cells fabricated using a nematic LC and rubbed polymer films created from *n*-alkylsulfonylmethyl- and *n*-alkylthiomethyl-substituted polystyrenes exhibiting more than 8 carbons (number of alkylcarbon > 8) display vertical LC alignment behaviors.[58] The LC cells created from the 4-alkylphenoxymethyl-substituted polystyrenes exhibit vertical LC alignment behaviors even at a very high rubbing density.[61]

However, synthetic polymers, such as polyimide, exhibiting stable LC alignments, can be regarded as a cause of environmental pollution due to their low degradability.[62] Especially, there are critical issues for use of polyimide as LC aligning materials. The hard baking process is essential in producing polyimide orientation layers. In general, it is thermally processed at temperatures above 200 °C, which is a high temperature for the practical manufacture of flexible plastic products.[63,64] Recently, the importance of eco-friendly materials has been recognized, thus, natural polymers are considered as alternatives to replace synthetic polymers for various applications due to their low cost, high availability, and low toxicity as well as their renewability/sustainability, biodegradability, biocompatibility, and thermostability.[65-68] The LC alignment behavior of the LC cells, created from rubbed cellulose films, which exhibit a homogeneous planar LC alignment for display applications has been investigated.[69,70] To the best of our knowledge, there are presently no reports on vertical LC alignments on thin films of cellulose and its derivatives.

Guar gum, which is an easily available galactomannan, exists as a natural polysaccharide extracted from *Cyamopsis tetragonoloba* seeds.[71] Guar gum is composed of a chemical structure of polysaccharides consisting of a mannose backbone with galactose side groups.[72] The backbone is a linear chain of β-1,4-linked *D*-mannose units to which galactose units are α-1,6-linked at every second mannose, thus forming bulky side branches.[73]

In this study, the LC alignment behavior of the LC cells produced using a plant-based guar gum film as an alignment layer is studied. The vertical LC alignment layers are produced from a LC cell fabricated with a guar gum film using the rubbing process. The optical and surface properties of the carefully treated guar gum films and the optical characteristics of the LC cells fabricated with the guar gum films are also studied. To the best of our knowledge, this is a pioneer study of the LC alignment behavior using guar gum films for eco-friendly LC display applications.

Experimental

1. Materials and instrumentation

Guar gum, which is a polysaccharide derivative, was purchased from Tokyo Chemical Industry Co., Ltd. Lithium chloride (LiCl) was obtained from Sigma Aldrich Co. Nematic liquid crystals, MLC-2086 (n_e = 1.5958, n_o = 1.4899, and $\Delta\varepsilon$ = 11.8) and MLC-6608 (n_e = 1.5586, n_o = 1.4756, and $\Delta\varepsilon$ = -4.2) was kindly donated and 4-*n*-pentyl-4'-cyanobiphenyl (5CB) (n_e = 1.7360, n_o = 1.5442, and $\Delta\varepsilon$ = 14.5) was purchased from Merck & Co., where n_e, n_o, and $\Delta\varepsilon$ represent the extraordinary refractive index, ordinary refractive index, and dielectric anisotropy, respectively. Ethanol (Dae-Jung Chemicals & Metals Co., Ltd.) was dried over molecular sieves (4 Å).

The optical transmittance of the polymer films onto glass substrates was obtained using ultraviolet-visible (UV-Vis) spectroscopy (MECASYS Co. Ltd., OPTIZEN POP). The contact angles of distilled water and diiodomethane with respect to the polymer films were determined with a contact angle measuring system (Krüss GmbH, FM40 EasyDrop) equipped with a drop shape analysis software. The surface energy value was calculated using the Owens-Wendt's equation based on the contact angle measurements of two standard liquids in contact with a solid surface as given below,

$$\gamma_{sl} = \gamma_s + \gamma_l - 2(\gamma_s^d \gamma_l^d)^{1/2} - 2(\gamma_s^p \gamma_l^p)^{1/2}$$

where γ_l is the surface energy of the liquid, γ_s^l is the interfacial energy of the solid/liquid interface, γ_s is the surface energy of the solid, γ_l^d and γ_l^p are known for the test liquids, and γ_s^d and γ_s^p can be calculated from the measured static contact angles.[74] The polarized optical microscopy (POM) images of the LC cell were obtained using an optical micro-

scope (Olympus, BX51) equipped with a polarizer and digital camera (Tucsen Photonics, ISH300). The voltage holding ratio (VHR) was measured using a VHR measurement system (autronic-MELCHERS, VHRM 105). The pulse width, frame frequency, and data voltages were 64 μs, 60 Hz, and 1.0 V, respectively. The measurement temperatures were 25 °C and 60 °C. The residual DC voltage (R-DC) value was evaluated using the capacitance-voltage (C-V) hysteresis method, which is used by Nissan Chemical Industries Ltd.

2. Preparation of films and LC cell assembly

Guar gum, which is a polysaccharide derivative, was used as a polymer film (Figure 1). We prepared a guar gum solution in ethanol/LiCl solution at 50 °C for 24 h. This solution was filtered using a polytetrafluoroethylene (PTFE) membrane with a pore size of approximately 0.45 μm. Thin films of guar gum were prepared by spin-coating (2000 rpm, 60 s) the gum onto glass substrates. Polyimide (PI, Nissan Chemical SE-7492K) alignment agents were spin coated (3000 rpm, 40 s) onto glass substrates. The PI films were pre-baked at 80 °C for 15 min and then were fully baked at 220 °C for 45 min. These polymer films were rubbed using a rubbing machine (RU-AS01, SHINDO Eng.); number of rubbing was 1 and rubbing depth was 0.1, 0.2, 0.3, 0.4 and 0.5 mm, respectively. The LC cells were fabricated using the polymer film onto both glass slides. The LC cells were constructed by assembling the films together using spacers with a thickness of 4.25 μm. The cells were filled with various nematic LCs consisting of a positive $\Delta\varepsilon$ LC mixture (MLC-2086), negative $\Delta\varepsilon$ LC mixture (MLC-6608), and positive $\Delta\varepsilon$ pure LC molecules (5CB), in the isotropic state to avoid creating a flow alignment due to capillary action. The LC cells manufactured using the guar gum were sealed with epoxy glue.

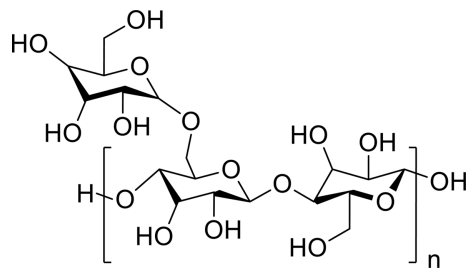

Figure 1. Chemical structure of plant-based guar gum.

Results and Discussion

1. Transmittance of guar gum films

Quantitative analysis of the transmittance of the plant-based guar gum films was performed using ultraviolet-visible (UV-Vis) spectroscopy to investigate the possibilities of surface coating applications (Figure 2). The traditional polyimide that is widely used as an alignment layer exhibits an electron conjugation structure, which results in an intrinsically yellowish coloration since a strong electron conjugation induces a high absorption of the red-light ranges of wavelength.[75,76] Therefore, conventional polyimides were not suitable for use in the experiment due to their transmittance characteristics. However, guar gum films are structurally free of electron conjugation and are thus, colorless and transparent. For example, the transmittance of a guar gum film is approximately 99% at a wavelength of 550 nm, which is significantly better than that (approximately 87%) of a polyimide film at the same wavelength, as previously reported by other research groups.[77,78] Conclusively, the optical transparency of a guar gum film in the visible light region is satisfactory for their use as electro-optical materials.

2. Liquid crystals (5CB, MLC-2086, and MLC-6608) alignment behaviors of the LC cells fabricated with guar gum films at same rubbing depth

The LCs alignment behaviors were determined by examining the photographic and conoscopic/orthoscopic polarized optical microscope (POM) images of the LC cells fabricated with the guar gum films, after the rubbing process using a

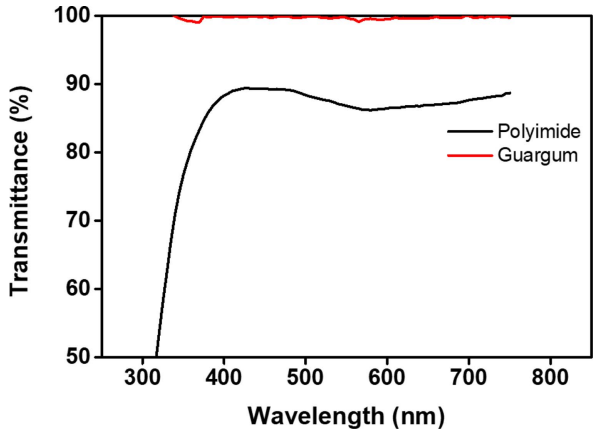

Figure 2. Ultraviolet-visible (UV-Vis) transmittance spectra of guar gum and polyimide alignment layers onto glass substrates.

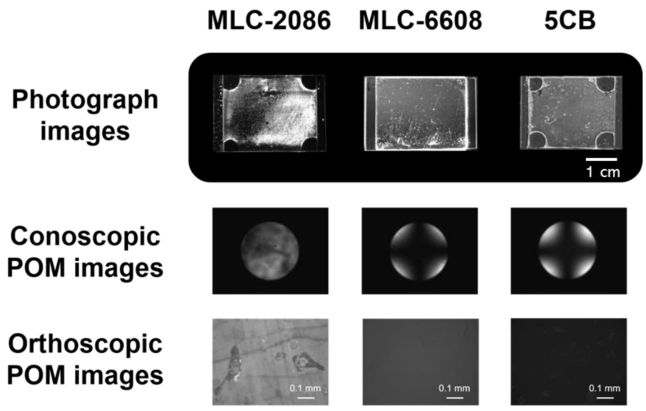

Figure 3. Photograph images of the LC cells fabricated with rubbed guar gum film by injection of various liquid crystals (MLC-2086, MLC-6608, and 4-*n*-pentyl-4'-cyanobiphenyl (5CB)) at a rubbing depth of 0.5 mm.

depth of 0.5 mm according to the type of LC, by injection of various nematic LCs such as a positive $\Delta\varepsilon$ LC mixture (MLC-2086), negative $\Delta\varepsilon$ LC mixture (MLC-6608), and positive $\Delta\varepsilon$ pure LC molecules (4-*n*-pentyl-4'-cyanobiphenyl (5CB)) (Figure 3). At first, the photographic and conoscopic/orthoscopic POM images of the LC cell injected with MLC-2086 were partially displayed as vertical LC textures with a Maltese cross pattern and as random planar LC textures with birefringence, indicating that the LC cell injected with MLC-2086 exhibited a partial vertical LC alignment behavior. However, the Maltese cross pattern of the LC cell injected with MLC-6608 and 5CB was observed in the entire area of the conoscopic POM images, which indicates a satisfactory vertical LC alignment behavior. When we compare the vertical LC aligning abilities of the LC cells injected with MLC-6608 and those injected with 5CB, the vertical LC aligning ability of the LC cell injected with 5CB is better than that of the LC cell injected with MLC-6608, as observed from the photographic and conoscopic/orthoscopic POM images of the LC cell.

3. Liquid crystal (5CB) alignment behavior of the LC cells fabricated with guar gum films according to rubbing depths

To closely investigate the LC alignment behavior dependent on the rubbing depth of the guar gum films, we also examined the photographic images of the LC cells created from the guar gum films using 5CB and the rubbing depths of 0, 0.1, 0.2, 0.3, 0.4, and 0.5 mm (Figure 4). The LC cells created from the guar gum films at the rubbing depths of 0, 0.1, 0.2, 0.3, and 0.4 mm demonstrate random planar LC textures with birefringence. However, a satisfactory uniformity of the vertical LC alignment behavior of the LC cells fabricated with the guar gum films with a rubbing depth of 0.5 mm was observed in the entire area of the photographic images of the LC cells. All of the LC cells fabricated with

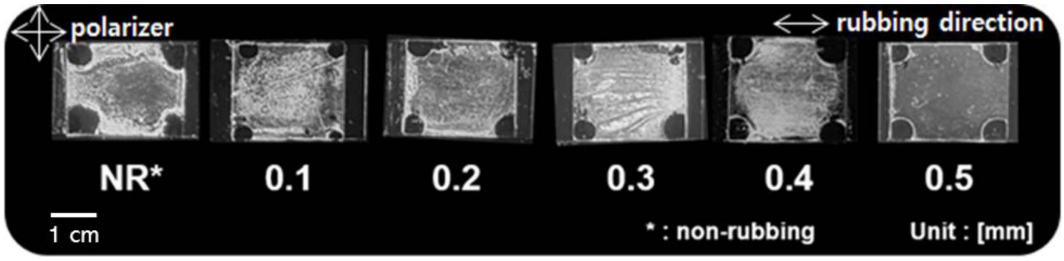

Figure 4. Photograph images of the LC cells fabricated with guar gum films according to the rubbing depth.

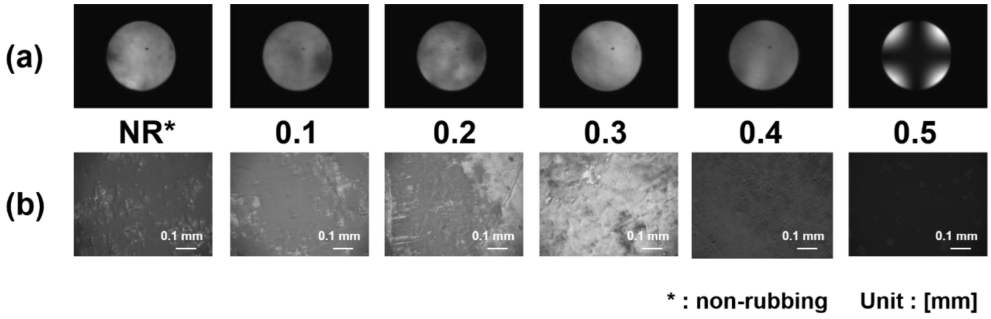

Figure 5. Polarized optical microscopy (POM) images of the LC cells made from guar gum films according to the rubbing depth; (a) Conoscopic POM images and (b) Orthoscopic POM images.

the guar gum films with the rubbing depth of 0.5 mm were able to produce stable and uniform vertical LC alignment layers and the vertical LC alignment was maintained for at least more than several months since we first created the LC cells from the guar gum films.

The LC alignment behaviors of the LC cells fabricated with the guar gum films and 5CB were investigated by observing the POM images (Figure 5). When the rubbing depth was less than 0.5 mm, the LC cells fabricated with the guar gum films exhibited random planar LC alignments with birefringence in the POM images. However, a homogeneous image with no birefringence in the orthoscopic image and a Maltese cross pattern in the conoscopic image of the LC cells fabricated using the guar gum films with the rubbing depth of 0.5 mm were observed, which indicate a vertical LC alignment. When the rubbing depth was larger than 0.5 mm, the LC cells fabricated with the guar gum films did not showed satisfactory vertical LC alignments due to the birefringence in the POM images (data not shown). Therefore, it was also found that the guar gum films were able to produce stable and uniform vertical LC alignment layers at the rubbing depth of 0.5 mm.

4. Surface properties of guar gum films according to rubbing depths

In order to investigate the correlation between the guar gum films and the LC molecules according to the rubbing depth, we calculated the surface energy values of the guar gum films according to the rubbing depths of 0, 0.1, 0.2, 0.3, 0.4, and 0.5 mm based on the static contact angles of water and diiodomethane (Table 1 and Figure 6). The total surface energy value, that is a summation of the polar and dispersion contributions, was calculated using the Owens-Wendt's equation based on the contact angle of two standard liquids, water and diiodomethane. We also found that there were critical surface energy values of the polymers exhibiting a vertical LC alignment behavior. As shown in Table 1, the dispersion and polar surface energy of the guar gum films according to the rubbing depths of 0, 0.1, 0.2, 0.3, 0.4, and 0.5 mm were measured in the ranges of 27.29-28.54 and 21.04-29.56 mJ/m^2, respectively. The total surface energy values of the guar gum films increased to 48.33, 52.23, 53.65, 54.98, 56.62, and 58.10 mJ/m^2 according to the rubbing depths. The dispersion surface energy values slightly increased to 27.29, 26.79, 27.92, 28.42, 28.68, and 28.54 mJ/m^2 according to the rubbing depths. The polar surface energy values of the guar gum films increased to 21.04, 25.44, 25.74, 26.56, 27.94, and 29.56 mJ/m^2 according to the rubbing depths. A vertical alignment behavior was observed in the LC cell fabricated with the guar gum films at the rubbing depth of 0.5 mm and the critical total surface energy of the guar gum films was 58.10 mJ/m^2. A vertical LC alignment is possible due to the total surface energy of the guar gum films, which indicates the presence of bulky galactose side chains on the surface of the guar gum films at the rubbing depth of 0.5 mm. We believe that the correlation of the polar surface energy to the liquid crystal alignment behavior is higher than its correlation to the dispersion surface energy, thus indicating that the polar surface energy is more critical to the vertical LC alignment as compared to the dispersion surface energy, as reported previously.[79-81] Conclusively, vertical LC alignment has been ascribed to the incorporation of a unique chemical structure of bulky galactose moieties into the side chains of the guar gum and the critical total surface energy originating from the discovery of unique saccharide groups at a specific rubbing

Table 1. Surface Energy Values and LC Alignment Properties of the Polymers

Rubbing depth (mm)	Contact angle (°)[a]		Surface energy (mJ/m^2)[b]			LC aligning ability[c]
	Water	Diiodo methane	Polar	Dispersion	Total	
0	56.4	49.2	21.04	27.29	48.33	X
0.1	50.2	48.7	25.44	26.79	52.23	X
0.2	48.7	46.3	25.74	27.92	53.65	X
0.3	47.0	44.9	26.56	28.42	54.98	X
0.4	44.7	43.9	27.94	28.68	56.62	X
0.5	42.3	43.6	29.56	28.54	58.10	O

[a]Measured from static contact angles.
[b]Calculated from Owens-Wendt's equation.
[c]Marks of circle (O) and cross (X) indicate polymer film have uniform vertical and partial vertical, planar LC aligning ability, respectively.

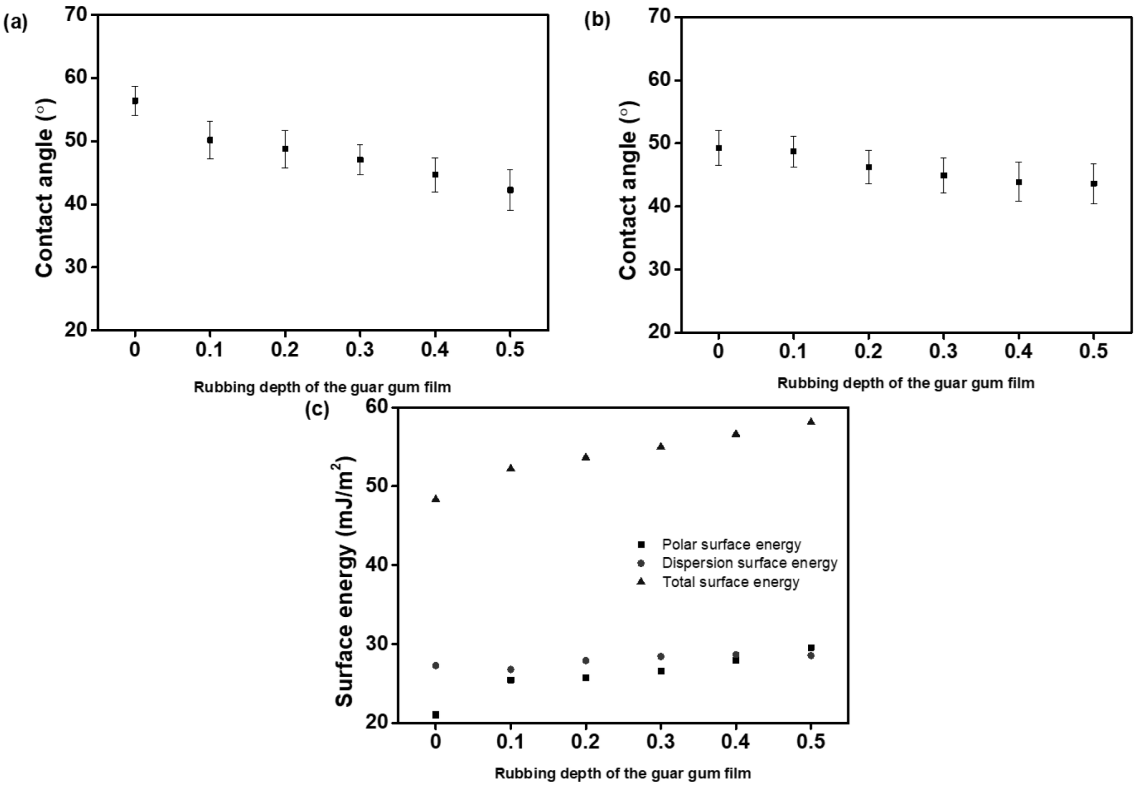

Figure 6. (a) Water, (b) diiodomethane contact angle, and (c) surface energy values of rubbed guar gum films.

strength.

5. Reliability and electro-optical performance of the LC cells fabricated with guar gum films

The reliability of the LC cells created from the polymer films was investigated by a stability test conducted to observe the LC alignment under severe environments such as ultraviolet (UV) irradiation and high temperature. At first, the UV stability of the LC cell created from the guar gum films with a rubbing depth of 0.5 mm was estimated from the POM image observed after the LC cells' exposure using UV irradiator (Artisan Technology Group, Spectronics XL-1500A) for 10 min, at 10, 20, 30, and 40 J/cm^2. As shown in Figure 7, the differences in the guar gum films exhibiting a vertical LC aligning ability cannot be observed from the Maltese cross pattern in the conoscopic POM images in the range of 0-40 J/cm^2, thus indicating that the vertical LC aligning ability of the guar gum LC cell is maintained at 40 J/cm^2. The thermal stability of the LC cells created from the guar gum films using the rubbing depth of 0.5 mm was estimated from the POM image observed at room temperature after heating the LC cells using hot plate for 10 min, at 100, 150, 200, and 250 °C. The differences in the guar gum films exhibiting a

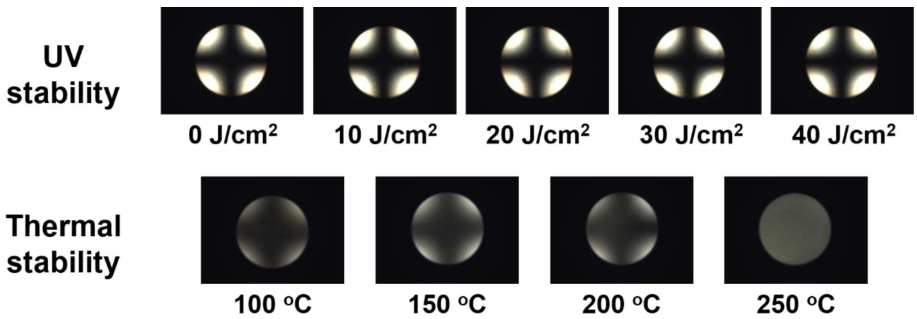

Figure 7. Conoscopic POM images of the LC cells made from guar gum films at rubbing depth of 0.5 mm; after UV irradiation treatment at 0, 10, 20, 30, and 40 J/cm^2 for 10 min and after thermal treatment at 100, 150, 200, and 250 °C for 10 min, respectively.

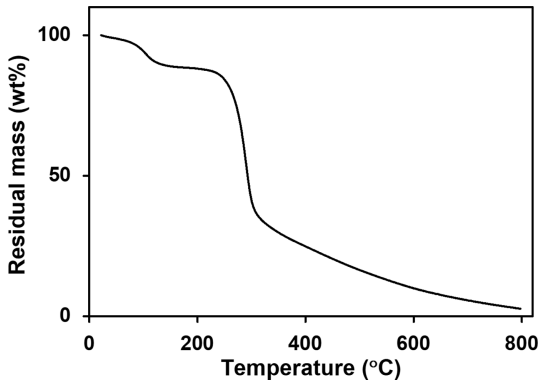

Figure 8. Thermogravimetric curve of guar gum.

vertical LC aligning ability cannot be observed from the Maltese cross pattern in the conoscopic POM images in the range of 100-200 °C, thus indicating that the vertical LC aligning ability of the guar gum LC cells is maintained even at 200 °C. The obtained total surface energy values of the guar gum films based on the static contact angles of water and diiodomethane were also measured after heating. When the temperature increases to 200 °C, the total surface energy value of the rubbed guar gum films is maintained at about 58 mJ/m^2. However, since the Maltese cross pattern of the conoscopic POM image disintegrates at 250 °C, the vertical LC alignment of the LC cells created from the guar gum films also disintegrates at 250 °C.

To analyze the thermal properties of guar gum, its pyrolysis behavior was measured up to 800 °C at a heating rate of 10 °C/min under an argon atmosphere. The thermogravimetric analysis (TGA) curve is shown in Figure 8. The first weight loss up to approximately 160 °C is due to the loss of the water absorbed by the guar gum. According to the thermogram, the total water content of the polymer is approximately 12 wt.%, and the thermal decomposition of the guar gum does not occur in the temperature range of 0-160 °C. The degradation process within the range of 230-300 °C, characterized by a weight loss of approximately 47 wt.%, is observed. This result may be ascribed to the loss of the degradation of the polymeric chain containing the primary hydroxy group in the guar gum.[82-84] The decomposed residues were fragmented to 800 °C, and finally exist as char at approximately 3 wt.%. The pyrolysis behavior of the guar gum can explain why the LC alignment layers created from the guar gum films do not maintain their vertical LC alignment behavior at 250 °C, as described in the previous paragraph.

The electro-optical (E-O) performance of the LC cell fabricated with the guar gum films was measured for possible practical LC device applications. The LC cell exhibited a voltage holding ratio (VHR) of above 99% at 25 °C and this value was maintained at 60 °C. It is sufficiently high for practical applications as the LC alignment layer in thin film transistors (TFTs) addressed LC devices. The residual DC voltage (R-DC) of the LC cell measured using the capacitance-voltage (C-V) hysteresis method was found to be very low at less than 15 mV, which is even smaller than that of commercial polyimides. This can provide a basic idea for the design of LC alignment layers based on renewable cellulose resources containing polymer films.

Conclusions

The liquid crystal (LC) alignment behaviors of LC cells fabricated with a polysaccharide such as guar gum were investigated. The guar gum films exhibited a satisfactory optical transparency in the visible light region (400-750 nm). For example, the transmittance value (99%) of the guar gum films onto a glass substrate at a wavelength of 550 nm is better than that (87%) of conventional polyimide films, which are the most commonly used LC alignment layers. The LC cells fabricated with the guar gum films exhibited different LC alignment behaviors according to various LC types. In addition, the LC cells created from the rubbed guar gum, that is a polysaccharide, exhibited a uniform vertical LC alignment after the alignment process with a rubbing depth of 0.5 mm. However, the LC cells created from the rubbed guar gum films with a rubbing depth of less than 0.4 mm exhibited a random planar LC alignment behavior. The uniform vertical alignment behavior exhibited a high correlation to the total surface energy values of the guar gum films having about 58.10 mJ/m^2. This study provides the fundamental information required for the design of LC alignment layers based on renewable and nature-based resources for electro-optical devices.

Acknowledgements

Financial supports by the Dong-A University Research Fund are gratefully acknowledged.

Conflict of Interest: The authors declare that there is no conflict of interest.

References

1. S. Chandrasekhar, "Liquid crystals", 2nd ed., Cambridge University Press, New York, USA, 1992.
2. R. B. Meyer, "Effects of electric and magnetic fields on the structure of cholesteric liquid crystals", *Appl. Phys. Lett.,* **12**, 281 (1968).
3. W. Brostow and H. E. H. Lobland, "Materials: Introduction and applications", John Wiley & Sons, New Jersey, USA, 2016.
4. R. Baetens, B. P. Jelle, and A. Gustavsen, "Properties, requirements and possibilities of smart windows for dynamic daylight and solar energy control in buildings: A state-of-the-art review", *Sol. Energ. Mat. Sol. C.,* **94**, 87 (2010).
5. H. Mori, Y. Itoh, Y. Nishiura, T. Nakamura, and Y. S. Y. Shinagawa, "Performance of a novel optical compensation film based on negative birefringence of discotic compound for wide-viewing-angle twisted-nematic liquid-crystal displays", *Jpn. J. Appl. Phys.,* **36**, 143 (1997).
6. H. K. Bisoyi and S. Kumar, "Liquid-crystal nanoscience: an emerging avenue of soft self-assembly", *Chem. Soc. Rev.,* **40**, 306 (2011).
7. S. J. Woltman, G. D. Jay, and G. P. Crawford, "Liquid-crystal materials find a new order in biomedical applications", *Nat. Mater,* **6**, 929 (2007).
8. T. Kato, M. Yoshio, T. Ichikawa, B. Soberats, H. Ohno, and M. Funahashi, "Transport of ions and electrons in nanostructured liquid crystals", *Nat. Rev. Mater.,* **2**, 1 (2017).
9. M. Kumar and S. Kumar, "Liquid crystals in photovoltaics: a new generation of organic photovoltaics", *Polym. J.,* **49**, 85 (2017).
10. J. Stöhr, M. G. Samant, A. Cossy-Favre, J. Diaz, Y. Momoi, S. Odahara, and T. Nagata, "Microscopic origin of liquid crystal alignment on rubbed polymer surfaces", *Macromolecules,* **31**, 1942 (1998).
11. M. Bremer, P. Kirsch, M. Klasen-Memmer, and K. Tarumi, "The TV in your pocket: development of liquid-crystal materials for the new millennium", *Angew. Chem.,* **52**, 8880 (2013).
12. J. F. Algorri, D. C. Zografopoulos, V. Urruchi, and J. M. Sánchez-Pena, "Recent advances in adaptive liquid crystal lenses", *Cryst.,* **9**, 272 (2019).
13. J. F. Algorri, P. Morawiak, N. Bennis, D. C. Zografopoulos, V. Urruchi, L. Rodríguez-Cobo, L. R. Jaroszewicz, J. M. Sánchez-Pena, and J. M. López-Higuera, "Positive-negative tunable liquid crystal lenses based on a microstructured transmission line", *Sci. Rep.,* **10**, 1 (2020).
14. M. Bosch, M. R. Shcherbakov, K. Won, H. Lee, Y. Kim, and G. Shvets, "Electrically actuated varifocal lens based on liquid-crystal-embedded dielectric metasurfaces", *Nano Lett.,* **21**, 3849 (2021).
15. N. Bennis, T. Jankowski, O. Strzezysz, A. Pakuła, D. C. Zografopoulos, P. Perkowski, J. M. Sánchez-Pena, J. M. López-Higuera, and J. F. Algorri, "A high birefringence liquid crystal for lenses with large aperture", *Sci. Rep.,* **12**, 1 (2022).
16. T. Onuma, E. Hosono, M. Takenouchi, J. Sakuda, S. Kajiyama, M. Yoshio, and T. Kato, "Noncovalent approach to liquid-crystalline ion conductors: high-rate performances and room-temperature operation for Li-ion batteries", *ACS omega,* **3**, 159 (2018).
17. Z. Ahmad, Z. Hong, and V. Viswanathan, "Design rules for liquid crystalline electrolytes for enabling dendrite-free lithium metal batteries", *Proc. Nat. Acad. Sci.,* **117**, 26672 (2020).
18. J. Beeckman, K. Neyts, and P. J. Vanbrabant, "Liquid-crystal photonic applications", *Opt. Eng.,* **50**, 081202 (2011).
19. Z. Zheng, H. Hu, Z. Zhang, B. Liu, M. Li, D. Qu, H. Tian, W. Zhu, and B. L. Feringa, "Digital photoprogramming of liquid-crystal superstructures featuring intrinsic chiral photoswitches", *Nat. Photonics,* **16**, 226 (2022).
20. Y. Gao, W. Ding, and J. Lu, "Templated Twist Structure Liquid Crystals and Photonic Applications", *Polymers,* **14**, 2455 (2022).
21. S. K. Gupta, D. Budaszewski, and D. P. Singh, "Ferroelectric liquid crystals: futuristic mesogens for photonic applications", *Eur. Phys. J.: Spec. Top.,* **231**, 673 (2022).
22. N. A. Gujarathi, B. R. Rane, and R. K. Keservani, "Liquid Crystalline System: A Novel Approach in Drug Delivery, in Novel Approaches for Drug Delivery", p. 190, Pennsylvania, USA, 2017.
23. P. Rajak, L. K. Nath, and B. Bhuyan, "Liquid crystals: an approach in drug delivery", *Indian J. Pharm. Sci.,* **81**, 11 (2019).
24. L. Nalone, C. Marques, S. Costa, E. B. Souto, and P. Severino, "Chapter 7 - Liquid crystalline drug delivery systems, in Drug Delivery Trends", ed. by R. Shegokar, p. 141, Elsevier, Amsterdam, Netherlands, 2020.
25. V. P. Chavda, S. Dawre, A. Pandya, L. K. Vora, D. H. Modh, V. Shah, D. J. Dave, and V. Patravale, "Lyotropic liquid crystals for parenteral drug delivery", *J. Controll. Release,* **349**, 533 (2022).
26. M. Chountoulesi, S. Pispas, I. K. Tseti, and C. Demetzos, "Lyotropic Liquid Crystalline Nanostructures as Drug Delivery Systems and Vaccine Platforms", *Pharmaceuticals,* **15**, 429 (2022).
27. C. Luan, H. Luan, and D. Luo, "Application and technique of liquid crystal-based biosensors", *Micromachines,* **11**, 176 (2020).
28. A. Parveen and J. Prakash, "Biosensing Using Liquid Crys-

tals", *Resonance,* **26**, 1187 (2021).
29. Z. Wang, T. Xu, A. Noel, Y. Chen, and T. Liu, "Applications of liquid crystals in biosensing", *Soft Matter,* **17**, 4675 (2021).
30. R. Qu and G. Li, "Overview of Liquid Crystal Biosensors: From Basic Theory to Advanced Applications", *Biosensors,* **12**, 205 (2022).
31. K. Takatoh, M. Sakamoto, R. Hasegawa, M. Koden, N. Itohand, and M. Hasegawa, "Alignment technology and applications of liquid crystal devices", Taylor & Francis, New York, USA, 2005.
32. K. Ichimura, "Photoalignment of liquid-crystal systems", *Chem. Rev.,* **100**, 1847 (2000).
33. J. Stöhr and M. G. Samant, "Liquid crystal alignment by rubbed polymer surfaces: a microscopic bond orientation model", *J. Electron. Spectrosc.,* **98**, 189 (1999).
34. M. Schadt, "Liquid crystal materials and liquid crystal displays", *Annu. Rev. Mater.,* **27**, 305 (1997).
35. A. Natansohn and P. Rochon, "Photoinduced motions in azo-containing polymers", *Chem. Rev.,* **102**, 4139 (2002).
36. M. Ree, "High performance polyimides for applications in microelectronics and flat panel displays", *Macromol. Res.,* **14**, 1 (2006).
37. J. H. Park, J. C. Jung, B. Sohn, S. W. Lee, and M. Ree, "Synthesis and characterization of novel polyimides containing stilbene unit in the side chain and their controllability of nematic liquid crystal alignment on the rubbed surfaces", *J. Polym. Sci. Pol. Chem.,* **39**, 3622 (2001).
38. H. Sakuma, "Potential energy surface of 4-hexyl-4′-cyanobiphenyl (6CB) on graphite surface: a DFT study with van der Waals corrections", *Mol. Simulat.,* **38**, 425 (2012).
39. H. Yu, J. Li, T. Ikeda, and T. Iyoda, "Macroscopic parallel nanocylinder array fabrication using a simple rubbing technique", *Adv. Mater.,* **18**, 2213 (2006).
40. M. F. Toney, T. P. Russell, J. A. Logan, H. Kikuchi, J. M. Sands, and S. K. Kumar, "Near-surface alignment of polymers in rubbed films", *Nature,* **374**, 709 (1995).
41. D. Seo and S. Kobayashi, "Effect of high pretilt angle for anchoring strength in nematic liquid crystal on rubbed polyimide surface containing trifluoromethyl moieties", *Appl. Phys. Lett.,* **66**, 1202 (1995).
42. Y. J. Kim, Z. Zhuang, and J. S. Patel, "Effect of multidirection rubbing on the alignment of nematic liquid crystal", *Appl. Phys. Lett.,* **77**, 513 (2000).
43. A. Lien, R. A. John, M. Angelopoulos, K. W. Lee, H. Takano, K. Tajima, and A. Takenaka, "UV modification of surface pretilt of alignment layers for multidomain liquid crystal displays", *Appl. Phys. Lett.,* **67**, 3108 (1995).
44. W. Lee, Y. S. Choi, Y. Kang, J. Sung, D. Seo, and C. Park, "Super-fast switching of twisted nematic liquid crystals on 2D single wall carbon nanotube networks", *Adv. Funct. Mater.* **21**, 3843 (2011).
45. J. Y. Ho, V. G. Chigrinov, and H. S. Kwok, "Variable liquid crystal pretilt angles generated by photoalignment of a mixed polyimide alignment layer", *Appl. Phys. Lett.,* **90**, 243506 (2007).
46. M. Liu, X. Zheng, S. Gong, L. Liu, Z. Sun, L. Shao, and Y. Wang, "Effect of the functional diamine structure on the properties of a polyimide liquid crystal alignment film", *RSC Adv.,* **5**, 25348 (2015).
47. M. Ghosh, "Polyimides: fundamentals and applications", 1st ed., Marcel Dekker, New York, USA, 1996.
48. M. B. Feller, W. Chen, and Y. R. Shen, "Investigation of surface-induced alignment of liquid-crystal molecules by optical second-harmonic generation", *Phys. Rev. A,* **43**, 6778 (1991).
49. N. Van Aerle and A. Tol, "Molecular orientation in rubbed polyimide alignment layers used for liquid-crystal displays", *Macromolecules,* **27**, 6520 (1994).
50. K. Lee, S. Paek, A. Lien, C. Durning, and H. Fukuro, "Microscopic molecular reorientation of alignment layer polymer surfaces induced by rubbing and its effects on LC pretilt angles", *Macromolecules,* **29**, 8894 (1996).
51. K. Weiss, C. Wöll, E. Böhm, B. Fiebranz, G. Forstmann, B. Peng, V. Scheumann, and D. Johannsmann, "Molecular orientation at rubbed polyimide surfaces determined with X-ray absorption spectroscopy: Relevance for liquid crystal alignment", *Macromolecules,* **31**, 1930 (1998).
52. R. Meister and B. Jérôme, "The conformation of a rubbed polyimide", *Macromolecules,* **32**, 480 (1999).
53. J. J. Ge, C. Y. Li, G. Xue, I. K. Mann, D. Zhang, S. Wang, F. W. Harris, S. Z. Cheng, S. Hong, and X. Zhuang, "Rubbing-induced molecular reorientation on an alignment surface of an aromatic polyimide containing cyanobiphenyl side chains", *J. Am. Chem. Soc.,* **123**, 5768 (2001).
54. D. Kim, M. Oh-e, and Y. R. Shen, "Rubbed polyimide surface studied by sum-frequency vibrational spectroscopy", *Macromolecules,* **34**, 9125 (2001).
55. K. E. Vaughn, M. Sousa, D. Kang, and C. Rosenblatt, "Continuous control of liquid crystal pretilt angle from homeotropic to planar", *Appl. Phys. Lett.,* **90**, 194102 (2007).
56. S. W. Lee, S. I. Kim, Y. H. Park, M. Reea, Y. N. Rim, H. J. Yoon, H. C. Kim, and Y. B. Kim, "Liquid-crystal alignment on the rubbed film surface of semi-flexible copolyimides containing n-alkyl side groups", *Mol. Cryst. Liq. Cryst. Sci. Technol. Sect. A-Mol. Cryst. Liq. Cryst.,* **349**, 279 (2000).
57. Y. J. Lee, Y. W. Kim, J. D. Ha, J. M. Oh, and M. H. Yi, "Synthesis and characterization of novel polyimides with 1-octadecyl side chains for liquid crystal alignment layers", *Polym. Adv. Technol.,* **18**, 226 (2007).

58. S. W. Lee, B. Chae, B. Lee, W. Choi, S. B. Kim, S. I. Kim, S. Park, J. C. Jung, K. H. Lee, and M. Ree, "Rubbing-induced surface morphology and polymer segmental reorientations of a model brush polyimide and interactions with liquid crystals at the surface", *Chem. Mater.,* **15**, 3105 (2003).
59. S. B. Lee, G. J. Shin, J. H. Chi, W. Zin, J. C. Jung, S. G. Hahm, M. Ree, and T. Chang, "Synthesis, characterization and liquid-crystal-aligning properties of novel aromatic polypyromellitimides bearing (n-alkyloxy) biphenyloxy side chains", *Polymer,* **47**, 6606 (2006).
60. H. Kang, J. S. Park, D. Kang, and J. Lee, "Liquid crystal alignment property of n-alkylthiomethyl-or n-alkylsulfonylmethyl-substituted polystyrenes", *Polym. Adv. Technol.,* **20**, 878 (2009).
61. H. Kang, T. Kim, D. Kang, and J. Lee, "4-Alkylphenoxymethyl-Substituted Polystyrenes for Liquid Crystal Alignment Layers", *Macromol. Chem. Phys.,* **210**, 926 (2009).
62. L. Chen, Y. Cao, T. Fang, W. Yue, J. Wang, X. Zhang, and F. Yang, "Synthesis and characterization of degradable polyimides from p-phenylenedioxybis (5-amino-2-pyridine)", *Polym. Degrad. Stab.,* **98**, 839 (2013).
63. Y. Zhang, C. Wang, W. Zhao, M. Li, X. Wang, X. Yang, X. Hu, D. Yuan, W. Yang, and Y. Zhang, "Polymer stabilized liquid crystal smart window with flexible substrates based on low-temperature treatment of polyamide acid technology", *Polymers,* **11**, 1869 (2019).
64. K. Ruan, Y. Guo, and J. Gu, "Liquid crystalline polyimide films with high intrinsic thermal conductivities and robust toughness", *Macromolecules,* **54**, 4934 (2021).
65. L. Hu, G. Zheng, J. Yao, N. Liu, B. Weil, M. Eskilsson, E. Karabulut, Z. Ruan, S. Fan, and J. T. Bloking, "Transparent and conductive paper from nanocellulose fibers", *Energy Environ. Sci.,* **6**, 513 (2013).
66. K. S. Mikkonen and M. Tenkanen, "Sustainable food-packaging materials based on future biorefinery products: Xylans and mannans", *Trends Food Sci. Technol.,* **28**, 90 (2012).
67. D. Das and A. Mukherjee, "Biomaterial film for soluble organic sorption and anti-microbial activity in water environment", *Bioresour. Technol.,* **110**, 412 (2012).
68. R. Zhao, P. Torley, and P. J. Halley, "Emerging biodegradable materials: starch-and protein-based bio-nanocomposites", *J. Mater. Sci.,* **43**, 3058 (2008).
69. H. Kang, J. Lee, B. Nam, and J. W. Bae, "Liquid crystal alignment behavior on transparent cellulose films", *RSC Adv.,* **5**, 38654 (2015).
70. J. W. Bae, E. Sohn, and H. Kang, "Liquid Crystal Alignment Behavior on Rubbed Films of Cellulose Acetate", *Mol. Cryst. Liquid Cryst.,* **626**, 215 (2016).
71. R. S. Banegas, C. F. Zornio, A. d. M. Borges, L. C. Porto, and V. Soldi, "Preparation, characterization and properties of films obtained from cross-linked guar gum", *Polímeros,* **23**, 182 (2013).
72. R. J. Chudzikowski, "Guar gum and its applications", *J Soc Cosmet Chem.,* **22**, 43 (1971).
73. V. D. Prajapati, G. K. Jani, N. G. Moradiya, N. P. Randeria, B. J. Nagar, N. N. Naikwadi. and B. C. Variya, "Galactomannan: a versatile biodegradable seed polysaccharide", *Int. J. Biol. Macromol.,* **60**, 83 (2013).
74. D. K. Owens and R. C. Wendt, "Estimation of the surface free energy of polymers", *J Appl Polym Sci,* **13**, 1741 (1969).
75. B. R. Bikson and Y. F. Freimanis, "Cause of the discolouration of aromatic polyimides", *Polym. Sci. (USSR),* **12**, 81 (1970).
76. F. Li, S. Fang, J. J. Ge, P. S. Honigfort, J. Chen, F. W. Harris, and S. Z. Cheng, "Diamine architecture effects on glass transitions, relaxation processes and other material properties in organo-soluble aromatic polyimide films", *Polymer,* **40**, 4571 (1999).
77. J. Cardoso, O. GomezDaza, L. Ixtlilco, M. Nair, and P. K. Nair, "Conductive copper sulfide thin films on polyimide foils", *Semicond. Sci. Technol.,* **16**, 123 (2001).
78. Y. Li, S. Fu, Y. Li, Q. Pan, G. Xu, and C. Yue, "Improvements in transmittance, mechanical properties and thermal stability of silica–polyimide composite films by a novel sol–gel route", *Compos. Sci. Technol.,* **67**, 2408 (2007).
79. S. Paek, C. J. Durning, K. Lee, and A. Lien, "A mechanistic picture of the effects of rubbing on polyimide surfaces and liquid crystal pretilt angles", *J. Appl. Phys.,* **83**, 1270 (1998).
80. B. S. Ban and Y. B. Kim, "Surface free energy and pretilt angle on rubbed polyimide surfaces", *J. Appl. Polym. Sci.,* **74**, 267 (1999).
81. H. Wu, C. Wang, C. Lin, R. Pan, S. Lin, C. Lee, and C. Kou, "Mechanism in determining pretilt angle of liquid crystals aligned on fluorinated copolymer films", *J. Phys. D Appl. Phys.,* **42**, 155303 (2009).
82. G. Dodi, D. Hritcu, and M. I. Popa, "Carboxymethylation of guar gum: synthesis and characterization", *Cell Chem. Technol.,* **45**, 171 (2011).
83. K. S. Soppirnath and T. M. Aminabhavi, "Water transport and drug release study from cross-linked polyacrylamide grafted guar gum hydrogel microspheres for the controlled release application", *Eur. J. Pharm. Biopharm.,* **53**, 87 (2002).
84. Y. Huang, J. Lu, and C. Xiao, "Thermal and mechanical properties of cationic guar gum/poly (acrylic acid) hydrogel membranes", *Polym. Degrad. Stab.,* **92**, 1072 (2007).